Supporting Information

Andrés et al. 10.1073/pnas.1320421111

SI Materials and Methods

Elemental X-Ray Analysis. To estimate the size of the vacuolar K^+ pool in in guard cells, freeze-fractured leaves of L14 plants grown in modified Long Ashton medium with 1 mM K^+ (LAK) were analyzed in a scanning electron microscope fitted with energy dispersive X-ray spectroscopy as described previously (1). Potassium contents in plant tissues were determined by measuring fresh and dry weight after drying samples at 70 °C for 48 h in a forced-air oven to obtain water contents (in grams of water per gram dry weight). Potassium was extracted by autoclaving finely ground material and then measured by atomic absorption spectrophotometry (1100B; Perkin-Elmer).

Gene Constructs and Transgenic Lines. The C terminus of the NHX2 and the N terminus of the GFP polypeptides were modified by PCR by using oligonucleotides NHX2-*Ngo*MIV (5′-ACCTCCGCCGGCAGGTTTACTAAGATC-3′) and GFP-*Ngo*MIV (5′-GCCGGCGGAGGTGTGAGCAAGGGCGAGG-3′). *Ngo*MIV digestion of amplified sequences and subsequent ligation generated an in-frame fusion of GFP to the C terminus of NHX2 that was cloned into the *Eco*RV site of the pBluescript polylinker. Next, the NHX2:GFP construct was moved as a 2998 bp XhoI-BamHI fragment to the plant transformation plasmid pBI321 (2). The C terminus of TIP1;1 and the N terminus of the GFP polypeptides were modified by PCR using oligonucleotides TIP-Not (5′-CCACCGCGGCCGCCGTAGTCTGTGGTTGGGAG-3′) and GFP-Not (5′-GCTGGCGGCCGCGGTGGTGTGAGCAAGGGCGAGGAGCTG-3′). NotI digestion of amplified sequences and ligation generated an in-frame fusion of GFP to the C terminus of TIP1;1. Plasmid pBI321Kan-TIP:GFP was constructed by cloning the TIP1;1:GFP translational fusion into pBI321 as a 1497 bp XhoI-BamHI fragment. Plasmids pBI321-Kan-TIP:GFP and pBI321-NHX2:GFP were used to transform Col-0 WT plants. Single-copy homozygous transformants in Col-0 were selected after three cycles of self-crossing from a T_1 population that exhibited a 3:1 segregation of the Kan^R marker. Null *nhx1 nhx2* mutant plants were recalcitrant to transformation and resistant to kanamycin as a result of the mutagenic transfer DNA insertions (1). Therefore, a hemizygote of genotype *nhx1-2*/*nhx1-2 NHX2*/*nhx2-1* was transformed with the pBI321Hyg-TIP:GFP plasmid carrying the hygromycin resistance marker. This plasmid was obtained by replacing the *NOS-NPTII-NOS* expression cassette of pBI321Kan-TIP:GFP with a *NOS-HptII-NOS* cassette using the ClaI/*Pme*I sites. Hygromycin-resistant segregants carrying the TIP1;1:GFP construct were screened by diagnostic PCR with allele-specific primers designed to amplify WT or mutant *NHX2* alleles to identify homozygous *nhx1-2 nhx2-1* null mutants. *Agrobacterium tumefaciens*-mediated transformation was according to a previous work (3), and transgenic plants were selected on half-strength Murashige and Skoog medium containing hygromycin (20 mg·L^{-1}) or kanamycin (50 mg·L^{-1}).

Semiquantitative RT-PCR. To study the transcriptional regulation of *NHX1* and *NHX2* genes along a day/night cycle, leaves of 6-wk-old Col-0 plants were harvested and frozen in liquid nitrogen at different time points: light onset, 2 h and 4 h of light, dusk, and 4 h in the dark. Total RNA from leaves was extracted by using TRIsure reagent according to the manufacturer's instructions (Bioline). Reverse transcription was performed on 1 μg of total RNA using the QuantiTect Reverse Transcription Kit following the manufacturer's instruction (Qiagen). PCR was performed with specific primers for *NHX1* (forward, 5′-GTATCTATGGCTCTTGCATACAAC-3′; reverse, 5′-ATCAAAGCTTTTCTTCCACGTTACCC-3′), *NHX2* (forward, 5′-CAGGGCACACAGAATTGCGCGGGAATG-3′; reverse, 5′-GTCACCATAAGAGGGAAGAGCAAG-3′), and *β-Tubulin-4* (*TB4*; forward, 5′-CAGTGTCTGTGATATTGCACC-3′; reverse, 5′-GACAACATCTTAAGTCTCGTA-3′). Densitometry analysis of the bands in ethidium bromide-stained agarose gels was performed with the software Quantity One (Bio-Rad). The ratio between the *NHX1/2* and *TB4* transcripts was calculated to normalize for initial variations in sample concentration. Mean and SE of the three replicas were calculated after normalization to *TB4*.

Real-Time RT-PCR. Total RNA was extracted from *Arabidopsis* leaves by using the RNeasy plant mini kit (Qiagen), and reverse transcription was performed on 1 μg of total RNA by using the QuantiTect Reverse Transcription Kit following the manufacturer's instructions (Qiagen). Real-time PCR was performed by using iTaq Universal SYBR Green Supermix (Bio-Rad), and the signals were detected on an iCYCLER (Bio-Rad). The cycling profile consisted of 95 °C for 10 min followed by 45 cycles of 95 °C for 15 s and 60 °C for 1 min. A melting curve from 60 to 90 °C was run following the PCR cycling to confirm the specificity of the primers. The expression levels of *NHX1* and *NHX2* genes were normalized to the constitutive *UBQ10* gene (*At4g05320*) by subtracting the cycle threshold (CT) value of *UBQ10* from the CT value of the gene (ΔCT). The fold change was calculated as $2^{-(\Delta CT\ mutant\ -\ \Delta CT\ WT)}$. The results shown are from three technical replicates of three independent RNA samples obtained from three different plants per genotype. Samples were obtained at two different time points of the day/night cycle from the same plants used for determining stomatal conductance of *nhx1-2* and *nhx2-1* single mutants. Primers user for quantitative RT-PCR were: *NHX1qRT* 5′- GAGGTCGTGGCTTTGTACCC-3′, *NHX1*rtR 5′- ATCAAAGCTTTTCTTCCACGTTACCC-3′, *NHX2qRT* 5′- GACTGAGAGAAGCAGCCATGA-3′, *NHX2*rtR 5′- GTCACCATAAGAGGGAAGAGCAAG-3′, *UBQ10F* 5′- GGCCTTGTATAATCCCTGATGAATAAG-3′, and *UBQ10R* 5′-AAAGAGATAACAGGAACGGAAACATAGT-3′.

1. Barragán V, et al. (2012) Ion exchangers NHX1 and NHX2 mediate active potassium uptake into vacuoles to regulate cell turgor and stomatal function in Arabidopsis. *Plant Cell* 24(3):1127–1142.
2. Martínez-Atienza J, et al. (2007) Conservation of the salt overly sensitive pathway in rice. *Plant Physiol* 143(2):1001–1012.
3. Clough SJ, Bent AF (1998) Floral dip: A simplified method for Agrobacterium-mediated transformation of Arabidopsis thaliana. *Plant J* 16(6):735–743.

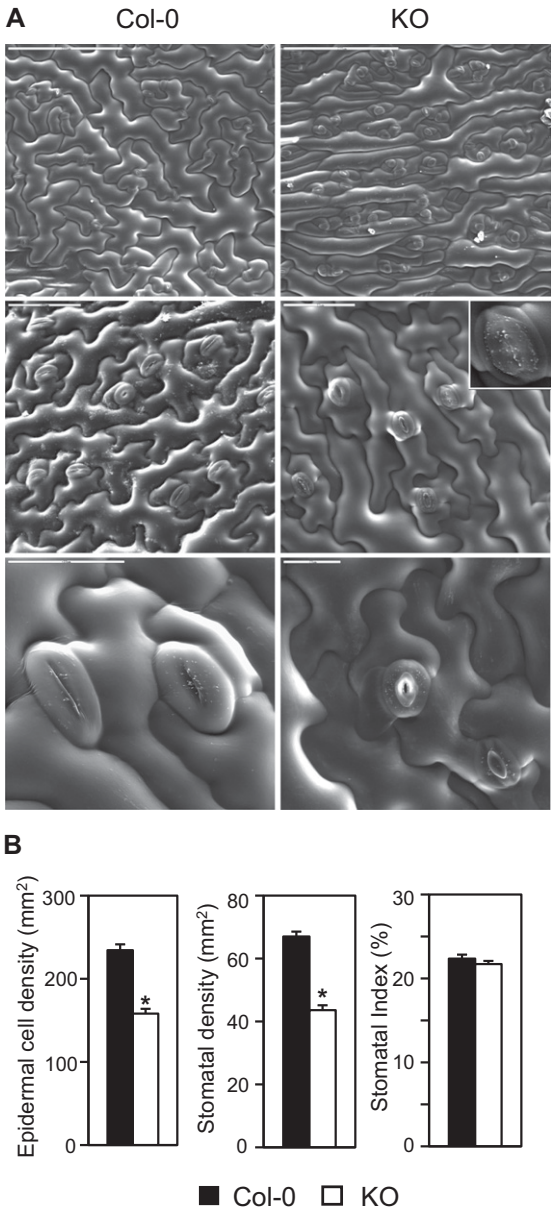

Fig. S1. Altered morphology of stomata and leaf epidermis in the *nhx1 nhx2* mutant. (*A*) Scanning EM images of leaves from *Arabidopsis* Col-0 and the KO line grown in hydroponic culture with LAK medium at 1 mM KCl. (*Top*) Appearance of the lower epidermis. (Scale bars: 200 μm.) Note the irregular distribution of cell sizes in the mutant. (*Middle*) Groups of stomata in the abaxial epidermis. (Scale bars: 50 μm) Note the deflated appearance of the stomata (*Inset*). (*Bottom*) Close-up images of stomata. (Scale bars: 20 μm.) (*B*) Epidermal cell density (*Left*), stomatal density (*Center*), and stomatal index (*Right*) calculated from dental resin impression images. Data represent means and SE from of least 42 images per line. Asterisks indicate statistically significant differences at $P < 0.05$ in pairwise comparison by Tukey HSD test.

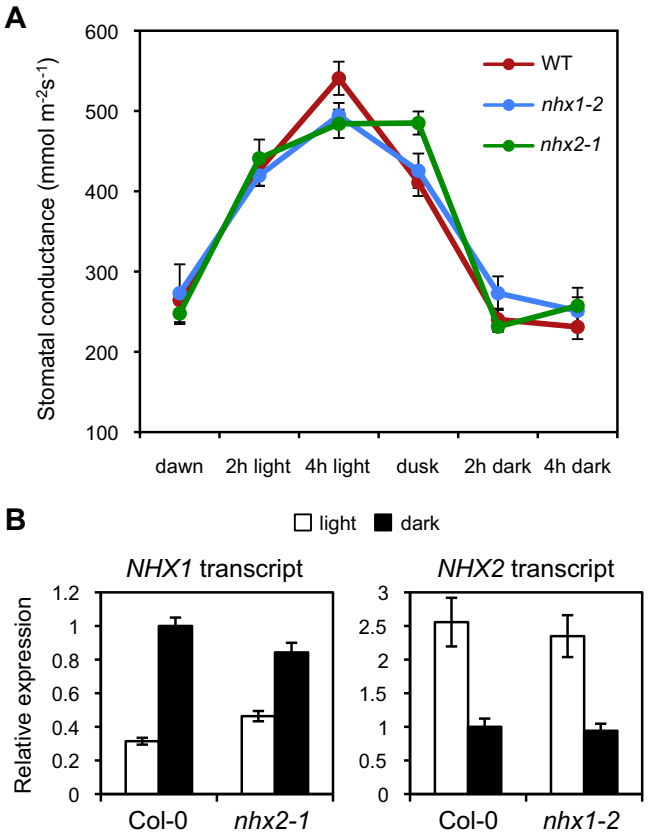

Fig. S2. Stomatal conductance and transcript abundance in single *nhx1* and *nhx2* mutants. (*A*) Stomatal conductance measurements in leaves of Col-0 and single mutant lines *nhx1-2* and *nhx2-1* at different time points of the day/night cycle. Dawn and dusk samples were collected 15 min before light was switched on and off, respectively. Data represent mean and SE of three plants per line. (*B*) Quantitative RT-PCR analysis of *NHX1* and *NHX2* mRNA expression levels in whole leaves at different time points of the day/night cycle. Samples were collected from plants shown in *A*, with three technical replicas each ($n = 9$), at time points 2 h after the onset of light and after 4 h in darkness. The transcript levels were normalized to the constitutive *UBQ10* gene. Data shown are means ± SE and represent the transcript levels of *NHX1* in the *nhx2-1* mutant plants and of *NHX2* in *nhx1-2* plants, relative to the transcript levels obtained for the WT Col-0 in the dark.

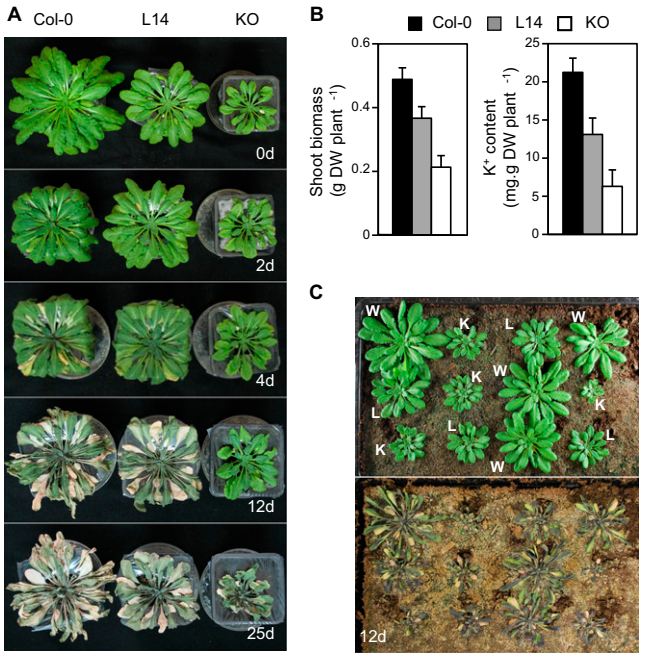

Fig. S3. Plant growth and K^+ content under water stress. (*A*) Col-0, L14, and KO plants growing in individual pots before treatment and after 2, 4, 12, and 25 d after drought stress. (*B*) Shoot biomass and K^+ content on a dry matter basis of WT plants (Col-0), the *nhx1-1 nhx2-1* mutant line (L14), and the *nhx1-2 nhx2-1* null mutant line (KO) grown in individual soil pots for 5 d without watering. The data correspond to plant samples (n = 3–4 plants per line) of the experiment shown in *A*. (*C*) Drought tolerance test of WT Col-0 (marked "W"), L14 (marked "L"), and KO plants (marked "K") growing in the same soil tray. Plants were grown for 6 wk in short day conditions (*Upper*) and then subjected to drought stress by ceasing watering for 12 d (*Lower*).

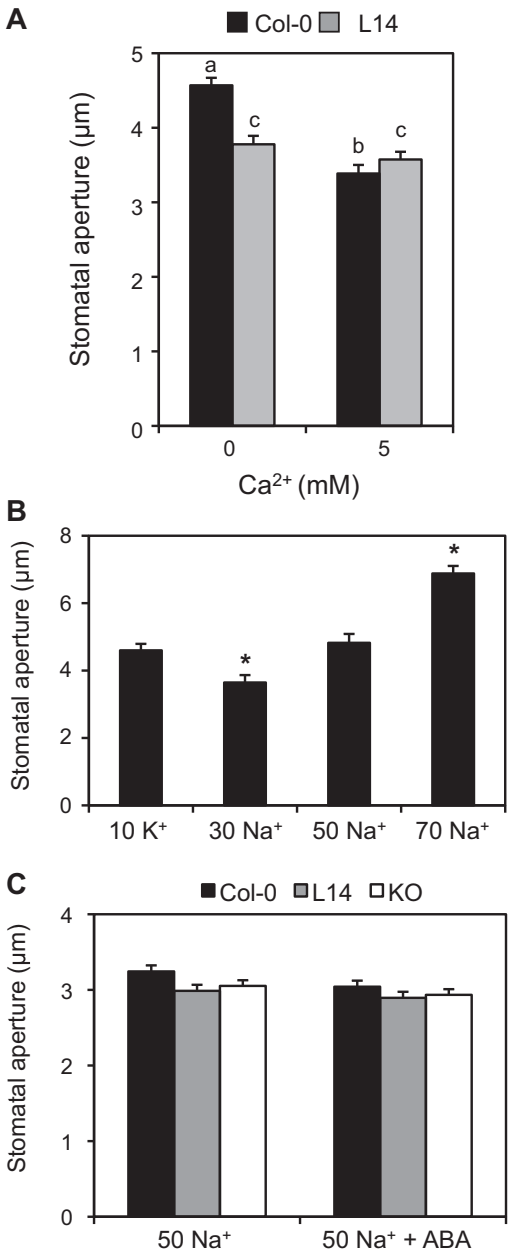

Fig. S4. Stomatal response to calcium and sodium salts. (*A*) Calcium-induced stomata closure. Data represent the mean and SE of the absolute values of aperture of at least 150 stomata per line and treatment. Letters indicate statistically significant differences between treatments for each line at $P < 0.001$ in pairwise comparison by Tukey HSD test. (*B*) Stomatal opening in the presence of sodium. Light-induced stomatal opening bioassays with WT Col-0 plants were conducted in buffers containing 10 mM KCl or NaCl at 30, 50, and 75 mM. Data represent the mean and SE of the stomatal apertures of at least 40 stomata per treatment. Asterisks indicate statistically significant differences relative to the K^+ treatment at $P < 0.001$ in pairwise comparison by Tukey HSD test. (*C*) Reversal of sodium-driven stomatal opening by abscisic acid (ABA). Light-induced stomatal opening in 50 mM NaCl for 4 h was followed by treatment with 1 μM ABA for an additional 1 h. Data represent the mean and SE of the stomatal apertures of at least 50 stomata per treatment.

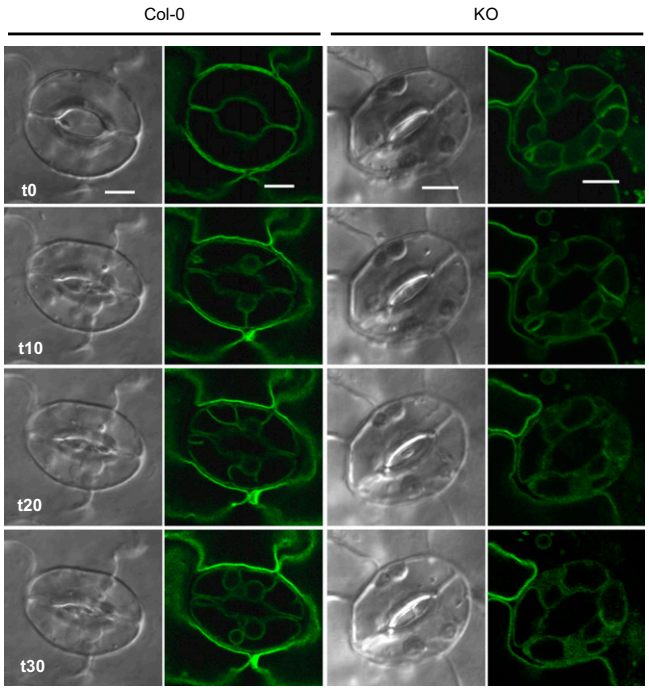

Fig. S5. Time lapse of vacuolar dynamics in leaf discs during stomatal closure. Vacuolar structure of Col-0 and KO guard cells visualized in leaf discs with TIP1;1:GFP at different time points after 10 μM ABA treatment. Bright-field (*Left*) and GFP images (*Right*) of TIP1;1:GFP. (Scale bar: 5 μm.)

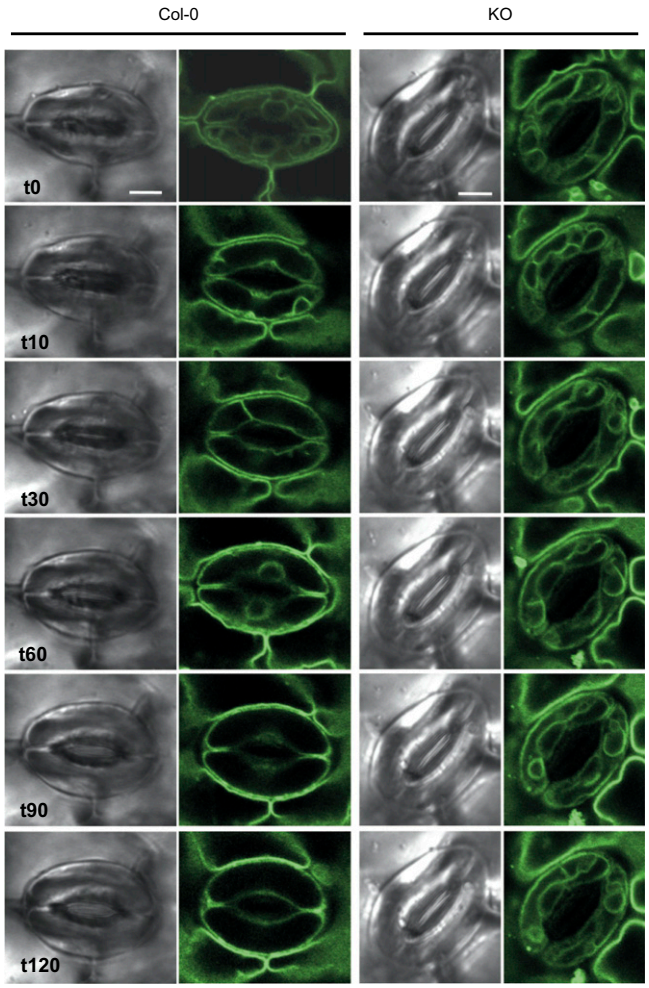

Fig. S6. Time-lapse of vacuolar dynamics in leaf discs during stomatal opening. Vacuolar structures in guard cells of Col-0 and KO plants visualized with TIP1;1:GFP at different time points after 3 μM fusicoccin treatment. Bright-field (*Left*) and fluorescence images (*Right*) of TIP1;1:GFP, respectively. (Scale bar: 5 μm.)

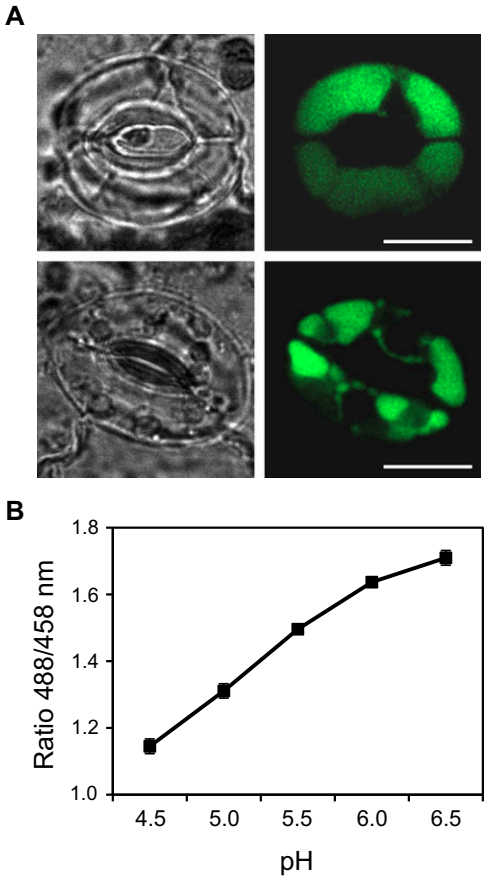

Fig. S7. Vacuolar compartmentation of the dye and ratiometric pH calibration curve. (*A*) Vacuolar lumen of open (*Upper*) and closed (*Lower*) WT stomata loaded with the pH-sensitive dye Oregon green. Bright-field (*Left*) and 488-nm–excited images (*Right*), respectively. (Scale bar: 5 μm.) (*B*) The mean ratios obtained from dividing the pixel density of 488-nm–excited images by the pixel density of 458-nm–excited images from guard cell vacuoles loaded with the pH-sensitive dye Oregon green were plotted against the pH of the equilibration buffer. Data represent means and SE from at least 20 stomata per treatment.

Table S1. Mean temperatures determined by thermal imaging of WT plants and *nhx1 nhx2* mutant lines at different day and night periods

Period (min)/line	Mean ± SD, °C	Paired differences mean ± SD, °C
P1 (40–170) day		
Col-0	20.822 ± 0.266	—
L14	20.880 ± 0.253	0.058 ± 0.022**
KO	21.110 ± 0.187	0.288 ± 0.084**
P2 (300–400) night		
Col-0	20.512 ± 0.229	—
L14	20.416 ± 0.226	0.097 ± 0.042**
KO	20.222 ± 0.171	0.290 ± 0.070**
P3 (600–700) night		
Col-0	20.522 ± 0.366	—
L14	20.429 ± 0.355	0.092 ± 0.037**
KO	20.158 ± 0.273	0.363 ± 0.111**
P4 (800–900) night		
Col-0	20.464 ± 0.363	—
L14	20.455 ± 0.353	0.009 ± 0.036*
KO	20.189 ± 0.272	0.276 ± 0.105**
P5 (950–1,050) night		
Col-0	20.406 ± 0.165	
L14	20.403 ± 0.170	0.002 ± 0.028^{ns}
KO	20.147 ± 0.126	0.259 ± 0.055**
P6 (1,100–1,227) day		
Col-0	20.984 ± 0.144	—
L14	21.073 ± 0.139	0.089 ± 0.019**
KO	21.197 ± 0.129	0.213 ± 0.069**

Statistical significance of differences in mean temperatures between the WT and mutant lines was determined by the Student *t* test. ns, no significant difference.
*$P < 0.05$ and **$P < 0.001$.